

Structure Analyses of Swollen Rubber-Filler Systems by Using Contrast Variation SANS

Mikihito Takenaka,^{*,†} Shotaro Nishitsuji,[†] Naoya Amino,[‡] Yasuhiro Ishikawa,[‡] Daisuke Yamaguchi,[§] and Satoshi Koizumi[§]

Department of Polymer Chemistry, Graduate School of Engineering, Kyoto University, Kyoto 615-8510, Japan, The Yokohama Rubber Company, Ltd., 2-1 Oiwaiki, Hiratsuka, Kanagawa 254-8601, Japan, and Advanced Science Research Center, Japan Atomic Energy Agency, Tokai, Ibaraki 319-1195, Japan

Received August 21, 2008; Revised Manuscript Received November 18, 2008

ABSTRACT: The polymer layers adsorbed on silica particles in rubber–silica systems have been investigated with the contrast variation small-angle neutron scattering (SANS) method. The scattering intensities of specimens swollen by solvents with various scattering length densities were measured. The contrast variation SANS for the specimens yielded partial scattering functions: the scattering function for polymer–polymer correlation $S_{pp}(q)$, the scattering function for silica–silica correlation $S_{ss}(q)$, and the scattering function for polymer–silica correlation $S_{ps}(q)$. The analyses of $S_{ss}(q)$ explored the hierarchical structures formed by silica particles. The analyses of $S_{ps}(q)$ and $S_{ss}(q)$ clarified the existence of dense polymer layers around silica aggregates. Several characteristic parameters are estimated from the analyses, such as the size of aggregates, the thickness of layers, the volume fractions of polymer of layers and matrix, and the correlation length of the matrix network. The contrast variation SANS is found to be a powerful tool for the analyses of the structures of the rubber–filler systems.

I. Introduction

Rubber–filler systems have been one of the most successful composite materials and have been widely used in industries such as tire and belts and so on.^{1,2} Fillers reinforce rubbers by compounding and improve the mechanical and barrier properties of the rubber compounds. The dispersion of filler particles in the rubber matrix is an important aspect of rubber reinforcement by fillers. In our previous studies,^{3,4} we investigated hierarchical structures formed by carbon black filler in polymers by using a combined ultra-small-angle and small-angle scattering method of neutrons and X-rays.

We need to explore another point in terms of structure analyses to clarify the correlation between the mechanical properties and the structures for rubber–filler systems: the adsorption of rubber in filler particles. For example, the rubber–silica systems with coupling agents exhibit much better mechanical properties than do those without the agent. However, little is known about how the polymers adsorbed on the silica particles. It is difficult to characterize the adsorption layer of polymers from the scattering of bulk systems because there is no contrast of scattering between the adsorption layers and the matrix phase of rubber. To clarify the adsorption layers, we shall investigate the swollen rubber–filler systems by using a solvent with a scattering technique. If the rubber is adsorbed on the filler surface by coupling agents, then the swollen ratio of the adsorbed layers will be smaller than that of the matrix phase, and the contrast of the scattering between the adsorption layers and the matrix phase is caused by the difference in the swollen ratio. In this article, we focus on a rubber–silica particles system as a rubber–filler system and characterize the adsorption layers on silica particles by using scattering. In the systems, there are three regions such as silica particles, adsorption layers, and matrix rubber, and the existence of the three regions makes the analyses of the scattering difficult. To

overcome this difficulty, we employ the contrast variation small-angle neutron scattering technique that is later described and characterize the adsorption layers as well as the aggregation of silica particles, network structures in matrix, and so on.

II. Experimental Methods

1. Samples. We used poly(styrene-*ran*-butadiene) (SBR; Nipol 1502, ZEON) as a rubber. The characterization of SBR is listed in Table 1. Silica particles (Zeosil 1165MP) used in this study were obtained from Rhodia. The silica particles were compounded into SBR by using a Banbury mixer at 80 °C, and they were then molded at 155 °C for 5 min. We made the sheets of SBR/silica particles with 1 mm thickness. The samples were swollen by a mixture of deuterated hexane (d-hex) and hexane (h-hex) with various composition. After reaching their equilibrium state (typically 12 h), we installed them in a quartz cell for further scattering experiments.

2. Small-Angle Neutron Scattering Measurements. We conducted SANS measurements with a SANS-J-II spectrometer at JRR-3 (Japan Research Reactor-3) in the JAEA (Japan Atomic Energy Agency, Tokai, Japan).⁵ The temperature of the samples was set to be 27 °C. The wavelength (λ) of the incident beam was 0.65 nm, and its distribution was 0.12. The scattered intensity was detected by a 2D ³He position-sensitive detector. The distances of the sample to the detector were 2.5 and 10.2 m, and thus the observed q range was from 0.07 to 0.8 nm^{−1}, where q is the magnitude of the scattering vector defined by

$$q = (4\pi/\lambda) \sin(\theta/2) \quad (1)$$

with θ being the scattering angle. The obtained scattering data were circularly averaged and corrected for background of cell, electronic noise of detector, detector sensitivity, and incoherent scattering.

3. Swelling Experiment. The specimens were swollen in hexane at 27 °C for 12 h to reach their equilibrium state, and their volume change was then measured. The degree of swelling in volume (Q)

Table 1. Characterization of SBR

polymers	M_w	M_w/M_n	w_{ps} (%) ^a	vinyl content (%) ^b
SBR	5.0×10^5	3.4	23.5	15

^a Weight fraction of styrene content. ^b Vinyl content in butadiene sequence.

* To whom correspondence should be addressed. E-mail: takenaka@alloy.polym.kyoto-u.ac.jp.

[†] Kyoto University.

[‡] The Yokohama Rubber Company, Ltd.

[§] Japan Atomic Energy Agency.

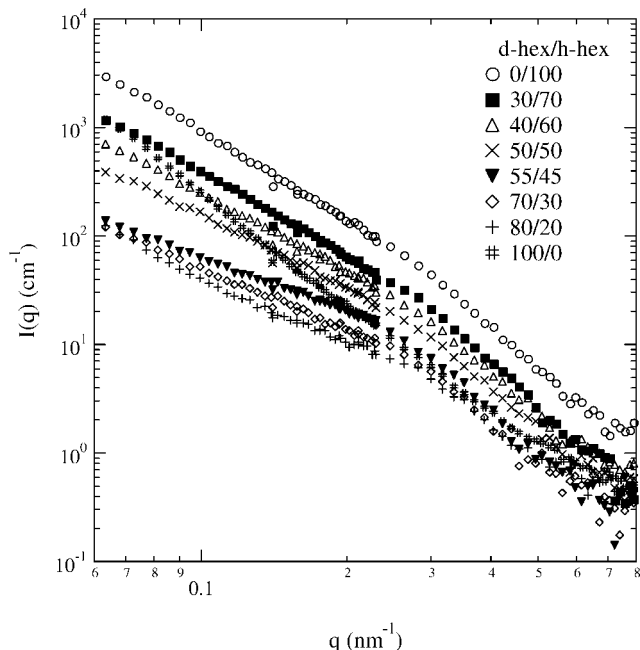


Figure 1. Scattering profiles for rubber-filler system swollen by d-hex/h-hex.

is calculated by $Q = V_S/V_0$, where V_0 and V_S are, respectively, the volumes before and after swelling.

III. Results and Discussion

Figure 1 shows the change in the scattering profiles $I(q)$ of the swollen rubber–silica system with the scattering length density of the solvent. The scattering intensity tends to decrease with h-hex. However, the scattering intensity increases at d-hex/h-hex = 100/0, and the q dependence of $I(q)$ changes with the scattering length density. These facts suggest that the swelling ratio of solvent to rubber is spatially inhomogeneous and that the network density has spatial fluctuations.

We analyzed the scattering profiles by using the contrast variation method developed by Endo.^{6–9} Because the volume fraction of minor components except for SBR and silica is <2 vol % in the swollen systems, the contribution of the minor components to the scattering intensity can be neglected. Therefore, the swollen rubber–silica system can be treated as three-component systems, and their scattering profiles can be described as follows under incompressible conditions

$$I(q) = (a_P - a_H)^2 S_{PP}(q) + (a_P - a_H)(a_S - a_H) S_{PS}(q) + 2(a_S - a_H)^2 S_{SS}(q) \quad (2)$$

Here a_i is the scattering length density of the i component (i : P, SBR; S, silica; H, hexane). $S_{ij}(q)$ is the partial scattering function defined by

$$S_{ij}(q) = \frac{1}{V} \int (\delta\phi_i(\vec{r}) \delta\phi_j(\vec{r}')) \exp[i\vec{q}(\vec{r} - \vec{r}')] d\vec{r} d\vec{r}' \quad (3)$$

where V is the scattering volume radiated by the incident beam and $\delta\phi_i(\vec{r})$ is the fluctuation of the volume fraction of i at position \vec{r} . In this experiment, we obtained the vector of scattering intensities $\vec{I} = [I_1(q), I_2(q), \dots, I_n(q)]$ from the same samples with n different scattering length densities of H . From eq 2, \vec{I} can be expressed as

$$\vec{I} = \mathbf{M} \cdot \vec{S} \quad (4)$$

where \mathbf{M} is the matrix of the difference in the scattering length density and \vec{S} is the vector of partial scattering functions. For three-component systems, \mathbf{M} is expressed by

$$\mathbf{M} = \begin{pmatrix} {}^1\Delta a_P^2 & 2 \cdot {}^1\Delta a_P \cdot {}^1\Delta a_S & {}^1\Delta a_S^2 \\ {}^2\Delta a_P^2 & 2 \cdot {}^2\Delta a_P \cdot {}^2\Delta a_S & {}^2\Delta a_S^2 \\ \vdots & \vdots & \vdots \\ {}^n\Delta a_P^2 & 2 \cdot {}^n\Delta a_P \cdot {}^n\Delta a_S & {}^n\Delta a_S^2 \end{pmatrix} \quad (5)$$

where

$${}^n\Delta a_P = a_P - {}^n a_H \quad (6)$$

and

$${}^n\Delta a_S = a_S - {}^n a_H \quad (7)$$

\vec{S} is given by

$$\vec{S} = \begin{pmatrix} S_{PP}(q) \\ S_{PS}(q) \\ S_{SS}(q) \end{pmatrix} \quad (8)$$

To decompose the scattering intensities into partial scattering functions, we need to calculate the transposed matrix \mathbf{M}^T satisfying $\mathbf{M}^T \cdot \mathbf{M} = \mathbf{E}$ by singular value decomposition. By applying \mathbf{M}^T to \vec{I} , \vec{S} can be obtained

$$\vec{S} = \mathbf{M}^T \cdot \vec{I} \quad (9)$$

Figure 2 shows the calculated partial scattering functions. $S_{PP}(q)$ and $S_{SS}(q)$ are positive, whereas $S_{PS}(q)$ is negative. If there is no adsorption layer and SBR is swollen by hexane homogeneously, then $S_{PS}(q)$ and $S_{PP}(q)$ are given by

$$S_{PS}(q) = -\phi_{\text{SBR}} S_{SS}(q) \quad \text{and} \quad S_{PP}(q) = \phi_{\text{SBR}}^2 S_{SS}(q) \quad (10)$$

and $S_{PS}(q)$ becomes negative, where ϕ_{SBR} is the volume fraction of polymer in the swollen network. Thus, the adsorption layer does not seem to exist. However, as shown in the plots of $S_{SS}(q)$, $S_{PP}(q)$, and $-S_{PS}(q)$ versus q on the double logarithmic scale in Figure 3, the q dependence of $-S_{PS}(q)$ is different from that of $S_{SS}(q)$ at lower q region, indicating that the swollen network is not spatially homogeneous.

To characterize the adsorption layer quantitatively, we calculated the scattering functions for the model consisting of the aggregation of silica particles (region α), the adsorption layers on the silica particles (region β) with the volume fraction of polymer (ϕ_1), and the matrix region (region γ) with the

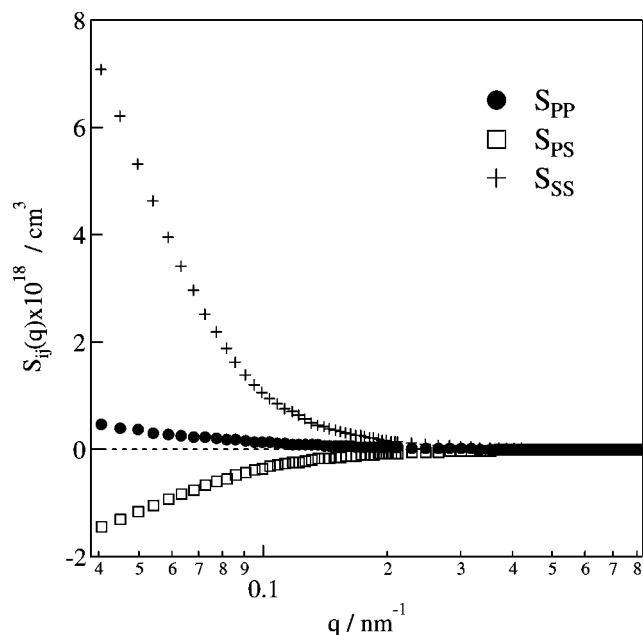


Figure 2. Partial scattering function of rubber-filler systems obtained from scattering profiles from Figure 1.

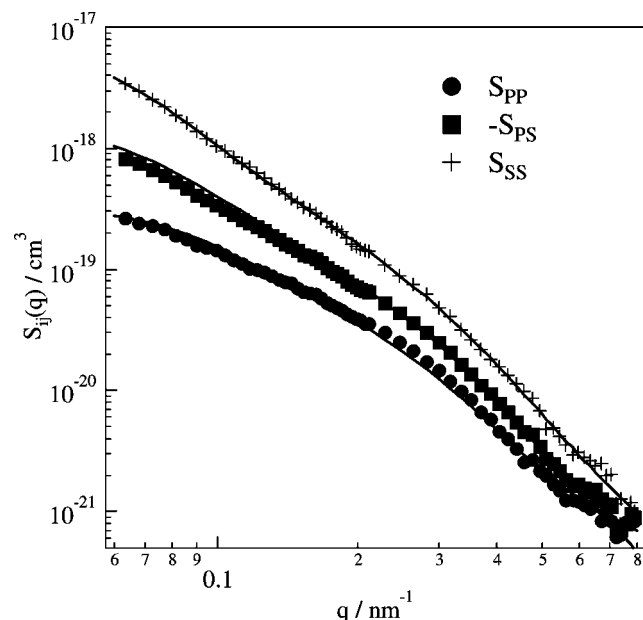


Figure 3. Partial scattering function of rubber-filler systems and their fitting results with model functions (solid lines).

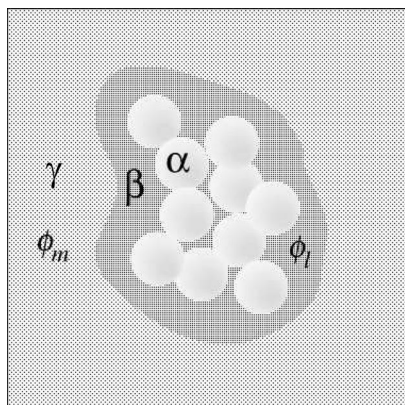


Figure 4. Schematic graph of the model of the rubber-silica system swollen by solvent.

volume fraction of polymer (ϕ_m), as shown in Figure 4. According to the model, the partial scattering function can be described by⁹

$$S_{SS}(q) = F_\alpha(q)^2 \quad (11)$$

$$S_{PS}(q) = (\phi_l - \phi_m)F_{\alpha+\beta}(q)F_\alpha(q) - \phi_l F_\alpha(q)^2 \quad (12)$$

$$S_{PP}(q) = [(\phi_l - \phi_m)F_{\alpha+\beta}(q) - \phi_l F_\alpha(q)^2] + S_{PP,th}(q) \quad (13)$$

where $F_\alpha(q)$ and $F_{\alpha+\beta}(q)$ are, respectively, the scattering amplitudes of region α and regions $\alpha + \beta$. The second term in the right-hand side of eq 13 expresses the concentration fluctuations originating from network structures in region γ . According to Sukumaran et al., the scattering of networks is given by¹⁰

$$S_{PP,th}(q) = S_{PP,th}(0) \left[\exp\left(\frac{q^2 \xi^2}{21.03}\right) + 0.541 \left(\frac{\xi^2}{7.01}\right) \times \left[\left\{ \text{erf}\left(\frac{q\xi}{\sqrt{6(7.01)}}\right) \right\}^3 / q \right]^{5/3} \right] \quad (14)$$

where ξ is the correlation length of the network. It should be noted that we neglected the higher level of extended tensile structure because the contribution of the higher level is much

Table 2. Composition of Samples Used in This Study

	SBR	silica	ZnO	stearic acid ^a	Si-69 ^b	sulfur	accelerator ^c
vol %	75.3	19.5	0.4	0.6	2.9	0.5	0.8

^a CH₃(CH₂)₁₆COOH. ^b Bis[3-(triethoxysilyl) propyl]tetrasulfide. ^c TBBS: *N-tert*-butyl-2-benzothiazyl sulfenamide.

Table 3. Scattering Length Density of Each Component Used in This Study

	hexane	d-hexane	SBR	silica
a_i (cm ⁻²)	-5.76×10^{-9}	6.14×10^{-10}	7.33×10^{-10}	3.15×10^{-10}

less than the scattering intensity originating from the inhomogeneity of the silica particle hole. The partial scattering function $S_{SS}(q)$ can be calculated by applying the mass fractal model that has an upper limit to the aggregation of silica particles^{11,12}

$$S_{SS}(q) = A \exp(-q^2 R_{g,a}^2/3) + B \left[\left\{ \text{erf}(q R_{g,a}/\sqrt{6}) \right\}^3 / q \right]^{D_f} \times (\exp(-q^2 R_{g,Si}^2/3)) + C \exp(-q^2 R_{g,Si}^2/3) + D \left[\left\{ \text{erf}(q R_{g,Si}/\sqrt{6}) \right\}^3 / q \right]^4 \quad (15)$$

where $R_{g,Si}$, $R_{g,a}$, and D_f are, respectively, the radius of gyration of silica particles, the radius of gyration of the aggregations, and the mass-fractal dimension of the aggregations.¹³ A , B , C , and D are expressed by¹⁴

$$A = n_a V_a^2 \quad (16)$$

$$B = (AD_f / c R_{g,a}^{D_f}) [\Gamma(D_f/2)] \quad (17)$$

$$C = n_{Si} V_{Si}^2 \quad (18)$$

$$D = 2\pi C S_{Si} / V_{Si}^2 \quad (19)$$

n_a , V_a , n , V_{Si} , S_{Si} , and c are, respectively, the number of aggregations per unit volume, the volume per unit volume, the number of silica particles per unit volume, the volume per silica particle, the surface area per silica particle, and the intrinsic dimension characterizing the degree of branching of the silica aggregation. The scattering function from regions $\alpha + \beta$ is expressed by an object with a sharp interface and a radius of gyration $R_{g,l}$ ¹¹

$$S_{\alpha+\beta}(q) = E \exp(-q^2 R_{g,l}^2/3) + G \left[\left\{ \text{erf}(q R_{g,l}/\sqrt{6}) \right\}^3 / q \right]^4 \quad (20)$$

where E and G are given by

$$E = n_a V_1^2 \quad (21)$$

$$G = 2\pi E S_{Si} / V_1^2 \quad (22)$$

where V_1 is the volume of regions $\alpha + \beta$. We fit the experimental partial scattering functions to the equation described above. The model functions can be well fitted to the experimental results, indicating that there are adsorption layers on the silica particles. The fitting results yielded the characteristic parameters. We listed them in Table 4.

First, we shall compare the volume fraction of polymer ϕ_m estimated from the SANS experiment with that from Q . The estimated value of Q is 2.54. Hexane cannot swell silica particles, but polymer chains. Thus, ϕ_m estimated from Q is given by

$$\phi_m = \frac{0.753}{0.753 + 2.54 - 1} = 0.33 \quad (23)$$

which agrees with $\phi_m = 0.32$.

Let us analyze the structure of the aggregation of silica particles. According to eqs 16 and 18 and the volume fraction

Table 4. Characteristic Parameters Yielded from Fitting

$R_{g,a}$ (nm)		D_f	$R_{g,l}$ (nm)	t_l (nm)	$R_{g, Si}$ (nm)	ξ (nm)	$S_{PP, th}(0)$
32.7		2.7	38.0	5.3	6.8	5.4	7.57×10^{-24}
ϕ_m	ϕ_l	A	B	C	D	E	G
0.32	0.61	1.18×10^{-17}	2.26×10^{-21}	1.30×10^{-19}	3.93×10^{-23}	1.18×10^{-17}	1.17×10^{-24}

of silica particles ϕ_{Si} in swollen rubber–silica systems, we can estimate V_a and V_{Si} from the following equations

$$V_a = \frac{A}{n_a V_a} = \frac{A}{\phi_{Si}} \quad (24)$$

and

$$V_{Si} = \frac{C}{n_{Si} V_{Si}} = \frac{C}{\phi_{Si}} \quad (25)$$

From the swelling experiment, $\phi_{Si} = 0.195/2.54 = 0.077$. By substituting ϕ_{Si} , A, and C into eqs 22 and 23, we obtained $V_a = 1.53 \times 10^{-16} \text{ cm}^3$ and $V_{Si} = 1.69 \times 10^{-18} \text{ cm}^3$, and there are 91 particles in an aggregation. However, it should be noted that the swelling may affect the structure of the aggregation of silica particles so that the obtained parameters for the aggregation may be different from those for the bulk system.

Finally, we shall estimate the molecular weight M_e between cross-linking from ξ . If we assume that hexane is a good solvent for SBR, then M_e is expressed by

$$M_e = M_0 \left(\frac{\xi}{l} \right)^{1.67} \quad (26)$$

where M_0 and l are, respectively, the molecular weight of a monomer of SBR and the statistical segment length of SBR. We substitute $M_0 = 65.9 \text{ g/mol}$ and $l = 0.7 \text{ nm}$ into eq 25, then we obtained $M_e = 2.0 \times 10^3 \text{ g/mol}$. We also calculated $M_e = 2.2 \times 10^3 \text{ g/mol}$ from the swelling experiment by using the Kraus equation¹⁵ with $Q = 2.54$ and an interaction parameter between SBR and hexane of 0.66. Both values agree well with each other.

IV. Conclusions

The polymer layers absorbed on silica particles in rubber–silica systems have been investigated with contrast variation SANS method. Specimens were swollen by the solvents with various scattering length densities and their SANS intensities were measured. We calculated the partial scattering functions by using singular value decomposition: the scattering function for polymer–polymer correlation $S_{PP}(q)$, the scattering function for silica–silica correlation $S_{SS}(q)$, and the scattering function

for polymer–silica correlation $S_{PS}(q)$. The analyses of $S_{PS}(q)$ and $S_{SS}(q)$ explored the existence of dense polymer layers around silica aggregates. $S_{SS}(q)$ reflects hierarchical structures formed by silica particles. To characterize the adsorption layer quantitatively, we calculated the scattering functions for the model consisting of the aggregation of silica particles, the adsorption layers on the silica particles, and the matrix region. We used the mass fractal model that has an upper limit for the aggregation of silica particles and an object with a sharp interface for the region's adsorption layers and silica aggregates to calculate the partial scattering functions. The model can express the experimental partial scattering functions well, and several characteristic parameters are estimated from the analyses, such as the size of aggregates, the thickness of layers, the volume fractions of polymer of layers and matrix, and the correlation length of the matrix network. The contrast variation SANS is found to be a powerful tool for the analyses of the structures of the rubber–filler systems.

References and Notes

- (1) Sternstein, S. *J. Macromol. Sci.* **1972**, B6, 243.
- (2) Koenig, J. L. *Acc. Chem. Res.* **1999**, 32, 1.
- (3) Koga, T.; Takenaka, M.; Aizawa, K.; Nakamura, M.; Hashimoto, T. *Langmuir* **2005**, 21, 11409.
- (4) Koga, T.; Hashimoto, T.; Takenaka, M.; Aizawa, K.; Amino, N.; Nakamura, M.; Yamaguchi, D.; Koizumi, S. *Macromolecules* **2008**, 41, 453.
- (5) Koizumi, S.; Iwase, H.; Suzuki, J.; Oku, T.; Motokawa, R.; Sasao, H.; Tanaka, H.; Yamaguchi, D.; Shimizu, H. M.; Hashimoto, T. *J. Appl. Crystallogr.* **2007**, 40, s474.
- (6) Endo, H. *Phys. Rev. Lett.* **2000**, 85, 102.
- (7) Endo, H. *J. Chem. Phys.* **2000**, 115, 580.
- (8) Endo, H.; Schwahn, D.; Cölfen, H. *J. Chem. Phys.* **2004**, 120, 9410.
- (9) Miyazaki, S.; Endo, H.; Karino, T.; Haraguchi, K.; Shibayama, M. *Macromolecules* **2007**, 40, 4287.
- (10) Sukumaran, S. K.; Beaucage, G.; Mark, J. E.; Viers, B. *Eur. Phys. J. E* **2005**, 18, 29.
- (11) Beaucage, G.; Schaefer, D. W. *J. Non-Cryst. Solids* **1994**, 172, 797.
- (12) Beaucage, G. *J. Appl. Crystallogr.* **1996**, 29, 134.
- (13) Beaucage, G. *J. Appl. Crystallogr.* **1995**, 28, 717.
- (14) Beaucage, G. *Phys. Rev. E* **2004**, 70, 031401.
- (15) Kraus, G. *Rubber Chem. Technol.* **1964**, 31, 6.

MA8019046